Interface energetics in zinc phthalocyanine growth on Ag(100)

Abdullah Al-Mahboob and Jerzy T. Sadowski

Phys. Rev. B **93**, 085413 — Published 8 February 2016

DOI: 10.1103/PhysRevB.93.085413

Interface energetics in zinc phthalocyanine growth on Ag(100)

Abdullah Al-Mahboob[1,2]*, and Jerzy T. Sadowski*[1,*]

[1]Center for Functional Nanomaterials, Brookhaven National Laboratory, Upton, NY 11973, USA

[2]Department of Physics, University of Liverpool, Liverpool, L69 3BX, UK

Keywords: organic self-assembly; low-energy electron microscopy; interface structure; structural phase transition; DFT calculations

Abstract

The nucleation and growth of zinc-phthalocyanine (ZnPc) thin films on Ag(100) surface are studied employing in situ, real-time low-energy electron microscopy (LEEM) and complementary DFT calculation to elucidate the role of incorporation kinetics of planar molecules in phase selection during nucleation, and apply this knowledge to fabrication of highly crystalline ZnPc films. We show that the nucleation of crystalline ZnPc islands requires a large concentration of diffusing molecules. The required amount of nominal deposition to initiate growth of ML high 2D crystalline islands is dependent on both, growth temperature and crystalline phase. At room temperature and slightly above (RT to ~430 K), ZnPc crystalline islands have double-domain R33.69 structure, with average domain size in sub-micrometer range. At higher temperatures, a 5x5 commensurate ZnPc structure nucleates. DFT calculations reveal significant differences in interfacial energies of an isolated ZnPc molecule on substrate, depending on an adsorption site and azimuthal orientation of the molecule relative to the substrate atomic lattice. The observed delay in the onset of the nucleation of an island is caused by existence of a large energy barrier for molecule incorporation into an island. At certain growth conditions it is possible to induce a structural transition from 5x5 to R33.69 phase, when the nominal coverage reaches 1ML. The resulting film has excellent crystallinity, with individual domains of hundreds of micrometers in size.

1. Introduction

Multidisciplinary research in organic molecular films draws significant attention due to synthetic flexibility, diverse functionality and progress in the field of organic devices, offering a potential for low cost, facile manufacturing. Among organic molecules, metal-phthalocyanines (MPc) are of continued interest, as they find both technological and scientific attention [1], being successfully used in various applications, such as plastic electronics [2], chemical sensors [3] and solar cells [4], to name a few. Metal-phthalocyanines belong to a class of macrocyclic compounds, with four nitrogen atoms which act as coordination centers for a metal ion within the central cavity of the MPc molecule. Pc form complexes with majority of elements in the periodic table [5] and thus they offer great flexibility for tuning their properties via changing the center metal ion and/or inserting different chemical end groups in the molecule. Metal center in MPc introduces various functionalities that make them useful in catalysis [6-8], gas sensing [9-11] and molecular magnetism applications [12]. Moreover, one of the most important advantages of phthalocyanines over other organic materials is their exceptional thermal and chemical stability. Thin films can therefore readily be prepared by organic molecular beam epitaxy (OMBE) in vacuum [13].

Unlike inorganic semiconductors, in which the interatomic forces arise from strong covalent or ionic bonds, MPc molecules are held together in a crystal or molecular film by weak van der Waals forces. This produces a variety of metastable polymorphs, depending on the preparation conditions of the film [1, 14-16]. In addition to the intermolecular interactions, film morphology is determined by the details of the interactions of the molecules with the substrate. The shape anisotropy of a planar molecule such as phthalocyanine is expected to make its aggregation processes complex, in a similar fashion to film growth of other anisotropic molecules [17-20]. Moreover, the metal center is accessible from both sides of the molecular plane. Therefore, a choice of metal center in the molecule determines not only the chemical functionality, but also opens the way for manipulating the interplay between molecule-molecule and molecule-substrate interactions, and thus controlling the resulting structure of a molecular film. For instance, 1ML CoPc grown on Ag(100) surface at RT is reported to have 5x5 commensurate structure with substrate lattice [21], while ZnPc on Ag(100) has been reported to have a double-domain structure [22]. Moreover, a gas phase (diffusing phase) CuPc on Au(111) surface at RT below 0.93 ML coverage and on Cu(111) below 0.76 ML coverage, respectively, are also reported [23]. In the present work, we examine the film growth of metal-Pc in relation to attachment-detachment kinetics for manipulating nucleation, phase transition and crystalline structures. In our primary study, we have deposited a number of metal-Pc on various substrates (oxides, graphene, 4-fold and 3-fold metal surfaces). Among these we have selected ZnPc and four-fold Ag(100) surface for extensive investigation, as a model system in which both, double domain and 5x5 commensurate structures are reported for RT grown MPc with Zn and Co metal center, respectively. Another reason of choosing (100) surface is that both of substrate and molecule have square symmetry. The MPc is a planar, rigid molecule, consisting of large number of atoms (49), strongly interacting with Ag surfaces [1]. Upon incorporation into a crystalline film, the molecule must assume a specific orientation and thus we expect that the anisotropy in rigid atomic arrangements and atomic bonding configuration within the molecule will result in a reorientation limited mechanism governing the growth of crystalline film [17-20].

2. Experimental and computational procedures

In this work we applied low-energy electron microscopy (LEEM) [24] as a main experimental technique, while complementary DFT calculations were employed for better understanding of the experimentally observed phenomena. LEEM and selected-area low-energy electron diffraction (μ-LEED) measurements were performed at the Elmitec SPE-LEEM system situated at beamline U5UA of the National Synchrotron Light Source. ZnPc was thermally evaporated on a single crystal Ag(100) substrate in the LEEM system under ultra-high vacuum, with base pressure in the range of $\sim 5\text{x}10^{-10}$ Torr, at deposition rates ranging from 0.03 to 0.05 ML/min. The molecular flux was calibrated monitoring the nominal deposition required for a full ML coverage of crystalline islands and further verified observing the additional nominal deposition required for completion of a 2nd layer. Here, 1 ML corresponds to 5.2×10^{17} molecules $\cdot$ cm^{-2} − the molecular density of a single crystalline layer composed of lying down ZnPc molecules at room temperature [22] that fully covers Ag(100) surface. The substrate temperatures were varied from RT to 520 K, depending on the experiment.

In order to better understand experimental results, the site-dependent and orientation-dependent interface energies of the ZnPc molecules on Ag(100), in-plane molecule-molecule binding energies (BE) and molecule-molecule interfacial energies were computed employing density functional theory (DFT). The DFT Electronic Structure Program Materials Studio DMol^3

[25, 26] has been employed. Geometry optimization and DFTD (GGA + dispersion correction) energy calculations were carried out by using Perdew-Bruke-Ernzerhof GGA functional [27] and van der Waals correction was accounted for by employing the dispersion correction for DFT (DFT-D method by Grimme) [28] using the DFT Semi-Empirical Dispersion Interaction Correction (DFT-SEDC) module [29]. The relativistic correction [30-31] was employed using VPSR pseudopotential [32]. The energies were calculated also for the optimized structure at local minima, in which azimuthal orientation and adsorption site of molecules were constrained.

The optimized adsorption site and molecule orientation for an isolated molecule was determined by placing it on a large, 4 atomic layers thick Ag(100) supercell (8x8) and subsequent geometry optimization. The interfacial energies were also calculated for the experimentally observed commensurate structure (5x5 phase). We did not perform similar calculations for the R33.69 phase, as a much larger unit cell for adsorption structure made the calculations not feasible. In order to get the relative interfacial energies, we have computed DFT-D binding energies of isolated ZnPc molecules on Ag(100) with various azimuthal orientations and their possible adsorption sites.

3. Results and discussion

We have studied structural evolution of zinc phthalocyanine (ZnPc) thin films on an Ag(100) single crystal, which can be regarded as a model system for phthalocyanine growth as we mentioned above. We utilized in investigating real-time nucleation and film-growth and phase transition varying substrate temperatures to elucidate how the energy barriers for incorporation (molecule diffusion and reorientation) affect the nucleation, growth and the resulting structure of the molecular film.

Upon deposition of ZnPc molecules on Ag(100) surface, we observed that a substantial nominal coverage of molecules is required before onset of the formation of crystalline ZnPc layer similar as reported ordered structure is determined by LEED upon coverage of CuPc over 0.76 ML and 0.93 ML on Cu(111) and Au(111) surfaces respectively [23]. Series of LEEM images recorded during deposition of ZnPc on Ag(100) kept at 375K is shown in Fig. 1. Note, that at this temperature the onset of nucleation of a crystalline ZnPc layer, manifested by appearance of "bright" islands in LEEM images, was observed at nominal coverage of 0.33ML. The selected-area low-energy electron diffraction (μ-LEED) pattern taken from the surface depicted in the first LEEM frame (Fig. 1a) is shown in Fig. 1d. The high background around the (00) diffraction spot and very faint diffraction features indicate that molecules are in a gas-phase, or transient state (transitional short range order) before the onset of nucleation of crystalline islands. Once they nucleate, the 1ML-high ZnPc islands have well defined crystalline structures and they are epitaxially aligned with Ag(100) substrate, as can be seen in Figs. 1e and 1f. From comparing these two LEED patterns it also becomes immediately apparent that changing the growth temperature results in different crystalline structure of the islands.

More detailed analysis of the LEED patterns revealed that at growth temperature of 375K the ZnPc film nucleates with double domain structure similar to one reported by Dou et al. [22]. Both LEEM data and μ-LEED pattern, which was obtained with a 2μm selected-area aperture (Fig. 2a) show that the individual domains are of sub-micron size. We utilized LEED pattern recorded from a clean Ag(100) surface, shown in Fig. 2c, as a reference for analysis of the ZnPc in-plane epitaxial structures. Every third ZnPc molecule matches its relative position with underneath Ag atom resulting in a unit cell (denoted subsequently "R33.69") with respect to the shortest Ag surface lattice vector described by Ag[0 ½ ½] and Ag[0 -½ ½]. The above described structure is obtained when ZnPc film is grown on substrate kept at temperatures from RT to approximately 445K.

When the substrate temperature exceeds 445K, a different LEED pattern is obtained, as shown in Fig. 2b. From the analysis of this pattern it is apparent that all the ZnPc islands have single commensurate orientation, but with about 4% larger in-plane lattice vectors (nearest neighbor distance, a = 14.445Å) in comparison with the double-domain structure (nearest neighbor distance, a = 13.89 ± 0.092Å). Lower molecular density of the 5x5 commensurate structure indicates that this is a substrate-induced structure. There, the position of neighboring ZnPc molecules matches with every 5^{th} Ag atom along shortest surface lattice vectors Ag[0 ½ ½], or Ag[0 -½ ½]. In further considerations we will label this phase as "5x5" phase.

As it is mentioned above, in real-time LEEM experiments we observe long delay in the nucleation of crystalline ZnPc islands. The nominal coverage of ZnPc molecules required to be on the substrate for the onset of nucleation increases with rise of substrate temperature. This critical coverage equals to 0.33ML at 375K, and it is as much as 0.87ML at 520K. In the literature, such delay in formation of an ordered layer is reported and described in terms of the interplay of intermolecular interaction and a large gas-phase concentration of molecules. In some specific cases, the high concentration of gas-phase is explained in terms of repulsive-attractive interaction versus intermolecular spacing at gas phase molecules [33]. However, those studies of delayed nucleation of ordered structure and prior high concentration of gas phase molecules [23.33] are lacking of information about concentration of diffusing molecules within the region in between crystalline islands after nucleation and during subsequent growth to complete a monolayer. As the LEEM allows to obtain spatially resolved information in real-time, we were able to monitor the coverage of crystalline islands as a function of total nominal deposition at given temperatures and deposition rates. The relation between nominal deposition and actual coverage of crystalline islands for these two temperatures is shown in Fig. 3. Interestingly, as we see in Fig. 3, the island grows faster than deposition rate, but coverage proceed linearly with time after nucleation, such that the gas-phase concentration in-between islands remains constant. This observation suggests a large critical concentration of gas phase molecules which are in kinetic equilibrium with the crystalline islands due to the balance between attachment and detachment processes.

If ZnPc is deposited on a substrate kept at higher temperature, nucleation of ordered island requires larger amount of nominal deposition. Therefore, one could speculate that the increase of critical coverage with the temperature is partially caused by desorption of ZnPc molecules at elevated substrate temperatures. This is not the case, however, as confirmed from both DFT calculation and the real-time LEEM experiments. Schematic landscape of relative interfacial energies obtained from DFT calculations is outlined in Fig. 4. DFT-calculated interface energy per molecule, between a molecule and Ag(100) surface is found to be 6.84 eV. Therefore we don’t expect any desorption at the growth temperatures presented in Fig 3. Moreover, we observed that virtually same nominal coverages (accounting for differences in the surface density of R33.99 and 5x5 phases) were required to grow full ML of ZnPc This supports our claim that there is no noticeable desorption of the ZnPc molecules at the range of substrate temperature employed. Reiterating, in the initial stages of the ZnPc deposition there is a large number of diffusing ZnPc molecules on the surface, which are in kinetic equilibrium (balancing kinetic attachment and thermal detachment against BE of molecules at the edge of nucleated island) with the nucleating island. In such case, the critical density required for onset of nucleation should depend on the substrate temperature and this relation should be governed by an Arrhenius type activation of detachment processes.

In classical nucleation and island growth theory, it is assumed that an ad-atom is attached immediately at an island edge just upon arrival. In the case of a molecular system, where the molecule has a different orientation in diffusing state than in crystalline state, if molecules require overcoming a large orientation barrier, it can result in a slow incorporation. In such cases, therefore, we have treated the problem in terms of incorporation-limited model, in which the molecules need to reorient themselves from time-averaged orientations in diffusing state to the one that matches the orientation of a molecule in the crystalline phase. This introduces an attachment barrier E_{at}. In our previous reports on growth of films made of anisotropic molecules [20,34], where the molecules prefer to be at different orientations at diffusive state (lying down) than that in crystalline islands (standing up), we found that the energy barrier for molecule reorientation causes a delay in the nucleation of crystalline islands. In that experimental system the incorporation-limited growth model was proposed. In the case of MPc on metal surfaces, molecules are lying down in both, the gas-phase and crystalline state, as this configuration maximizes total molecule-substrate interaction. However, the molecule should have a specific orientation in a crystalline film. We cannot exclude the existence of an energy barrier for molecule attachment in the growth of crystalline film, which originates from variation in interfacial energy depending on azimuthal orientation of the molecule. In fact, DFT calculation shows remarkable differences, up to few hundred meV, in both, the site-dependent and orientation-dependent BE, as shown in Fig. 4b. ZnPc molecules prefer to adsorb on hollow sites in Ag(100) lattice, with molecular axis rotated about $\pm 30^{\circ}$ in regard to [011] crystallographic direction of the substrate. This is in agreement with scanning tunneling microscopy (STM) data obtained from NiPc and CoPc molecules adsorbed on Ag(100) [35]. Molecule-substrate interaction (6.84eV/molecule obtained from DFT calculation for a commensurate polymorph) is much stronger than in-plane molecule-molecule interaction: 0.17eV for the 5x5 phase, 0.28eV for the R33.69 phase (without considering substrate in the calculations). It is also stronger than out-of-plane molecule-molecule interaction (0.94 eV). Increase in interfacial energies upon change in azimuthal orientation from 30^o to 15^o and 30° to 45° at a hollow site are 0.99 eV and 0.48 eV respectively. Actual energy barrier for azimuthal reorientation should be larger than that, as the reorientation process should occur through local transitional states. We can thus conclude that the reorientation barrier associated with anisotropy of molecular structure can be a prime factor over molecule-molecule interaction. This implies that an energy barrier for molecule reorientation should be considered in the analysis of film nucleation and growth. DFT calculations of site and orientation dependent adsorption energies of ZnPc molecules suggest a large effective energy barrier for a molecule being incorporated into a nucleus or an island. The nucleation and film growth should be considered in terms of incorporation limited kinetics. In such growth mechanism, only a fraction of molecules are attached upon their arrival at an island edge. Therefore, the concentration of gas-phase molecules at kinetic equilibrium is determined by the balance of a slow attachment and thermal detachment processes.

Neglecting the effect of deposition rate, a simplified rate of attachment, R_{at}, at in this incorporation limited mechanism can be given as:

$$R_{at} = \frac{1}{2} \rho p_a a v_{diff} \exp\left(-\frac{E_{at}}{k_B T} \right) \qquad (1)$$

Here E_{at} is the effective reorientation energy barrier averaged over all possible paths, ρ is the areal density of gas phase molecules, p_a is a capture perimeter, $a=\sqrt{\Omega}$ is the capture width (linear dimension of molecules); ν_{diff} is the thermal, or effective hopping frequency of diffusing molecules. Energy diagram, Fig. 4b, also suggest that energy barrier along diffusion path are smaller in comparison with barrier for azimuthal reorientation, therefore hopping between adsorption sites is faster than reorientation and thus exponential term in Eqn. 1 is the rate limiting factor at the growth temperature of interest. The rate of detachment is:

$$R_{det} = \rho_l \nu p_A \exp(-E_{det} / k_B T) \qquad (2)$$

Here ρ_l is the linear density of solid state molecules, ν is the statistical average frequency of vibrational mode (in-plane lattice mode) responsible in detachment, and p_A is the perimeter of the island/cluster within an area of interest A_0. In the kinetic equilibrium, $R_{at} = R_{det}$. The normalized kinetic equilibrium concentration, ρ/ρ_s at steady state is:

$$\rho_{norm}^{incrp} = \frac{\rho}{\rho_s} = \frac{2\nu p_A \rho_l}{\rho_s p_a \sqrt{\Omega}\nu_{diff}} \exp(-\Delta E / k_B T) = \frac{2\nu p_A}{p_a \nu_{diff}} \exp(-\Delta E / k_B T) \qquad (3)$$

$\rho_s == \rho_l \surd\Omega$ is the areal density of solid-state molecules just at an island edge, or a normalization constant in the experiments. The difference, $\Delta E = E_{det} - E_{at}$, is the energy barrier for molecule attachment. If the cluster size is large enough in comparison with dimension of molecule, which is the case of observable size of clusters/islands in LEEM mirror mode, the p_A/p_a is unity.

The incorporation limited nucleation of a growing island, thus, does not depend only on a formation of critical nucleus, but also requires reaching a critical concentration described by Eq. 3. Therefore a delayed observable nucleation occurs in this growth system, upon a nominal deposition required to reach a kinetic equilibrium of gas phase molecules and nucleated while in a classical nucleation and atomistic film growth mechanism, the nucleation of an island is stabilized by formation of a critical nucleus.

In one of the experiments, after deposition of about nominal 0.7ML of ZnPc at substrate temperature of 425K and observing the nucleation of crystalline islands, we increased the substrate temperature to 500K. The crystalline ZnPc islands gradually dissolved into the diffusive phase. After the substrate temperature was lowered again, we again observed nucleation of the ZnPc islands. When cooling down further after observing nucleation without any additional deposition, islands continued to grow (see supplementary movie) and the equilibrium concentration decreased as described by Eq. 3. Such heating-cooling cycles were repeated several times, and the final coverages of ZnPc crystalline phase at certain temperatures were observed to be the same as the one before first heating cycle.

We also have examined the temperature dependency of nominal coverage to initiate nucleation of an island driven by additional deposition required to reach kinetic equilibrium of gas phase molecules with a critical nucleus. Just upon observing the onset of growing island, the deposition was stopped, and substrate temperature was increased to dissolve the crystalline island into a gas phase. Subsequently, the deposition was continued with identical rate to observe next onset of nucleation of growing island at this higher substrate temperature. This procedure has been repeated to obtain critical coverage data versus substrate temperature. We found that the delays in nucleation of growing crystalline island for both phases, R33.69 and 5x5, are associated with a nominal coverage needed to reach kinetic equilibrium as described in Eq. 3. In the Fig. 5 the relation between critical coverage required for nucleation of crystalline islands and the growth temperature for both, R33.69 and 5x5 phases is shown. The activation barrier determining gas-phase concentration (inset in Fig. 5) is lower for the high temperature phase (single crystalline, 5x5), than for the low temperature phase (double domain structure, R33.69).

As mentioned above, 5x5 structure found at higher substrate temperatures is a substrate-induced single orientation commensurate phase and it is less dense than the R33.69 phase. We searched for the possibilities of achieving larger domain of R33.69 phase at high temperature and we looked at what happen upon increasing coverage beyond 1ML of 5x5 phase. In some cases we observed partial conversion to R33.69 phase, perhaps due to inefficient rearrangement of azimuthally anisotropic molecules in high coverage regime, where the surrounding molecules are in close proximity. Interestingly, when we continue to grow ZnPc at temperatures at, or above 475K, the 5x5 film converts to R33.69 phase when nominal deposition reaches 1 ML (in terms molecular density of R33.69 phase), as it is evident from μ-LEED patterns shown in Fig. 6. This further suggests that the 5x5 ZnPc structure is a substrate-induced phase and R33.69 phase is more bulk-like.

In our LEEM experiments, although we couldn't observe the initial site of the start of phase transition, samples were swept along XY position over 0.5 mm after observing phase transition in μ-LEED mode in LEEM. On surfaces with initial higher defect densities, we found that both R33.69 domains are present, with individual domain sizes in the range from about 10 μm to several hundred μm in diameter. With improving substrate quality, the individual domain sizes were larger – often approaching a 0.5 mm. Therefore we conclude that the phase transition usually starts from substrate defects and thus the nucleation density of R33.69 domains during phase transition from 5x5 structure is directly related to the initial substrate quality.

In the LEEM experiments we did not observe 3D growth of ZnPc at RT up to 6 ML nominal deposition. But in this case, single domain size of R33.69 is of sub-micrometer only. However, at higher temperatures the well-ordered layer by layer growth is sustained only up to 2 ML. Above that thickness ZnPc film becomes somewhat disordered, with appearance of 3D islands. Interestingly, when a giant R33.69 domain is grown at HT via the phase transformation described above, it is stable upon cooling; further deposition of ZnPc on this giant ML R33.69 domain at low temperatures results in layer by layer growth having identical domain orientation as of the first layer to at least 6 ML – a maximum thickness that we have studied in our current investigation so far.

4. Conclusions

In summary, we have reported here the film growth and coverage/temperature dependent phase transition processes of ZnPc on Ag(100) substrate observed in real time-LEEM and μ-LEED experiments complemented by understanding of interfacial energies obtained from DFT calculations. Our LEEM/LEED observation of film growth at substrate temperature ranged from RT to 520K revealed a delayed nucleation of crystalline ZnPc islands similar as reported for CuPc [23]. Temperature dependent real time concentration of gas phase molecules determined from LEEM experiments and computational support revealed that the kinetic equilibrium resulted from the balance of incorporation limited slow attachment of molecules and thermal detachment from island edge is responsible for such delay in nucleation of growing ML high 2D islands. Upon continued deposition crystalline phase continue to grow because of the excess deposition such that a high constant gas-phase concentration is maintained within inter-island spaces. We observed nucleation and growth of two crystalline phases. A double-domain structure with respect to substrate surface lattice orientation (labeled R33.69) is grown below 440K. This is similar as reported for ZnPc on Ag(100) in ref [22] and also expected as the overlayer have a mis-orientation of lattice vectors with respect to substrate and nucleation density is high even at low flux typically used in our experiments (order of 0.05 ML/min). Another phase is a substrate-induced single crystalline 5x5 commensurate structure, when grown above that temperature, identical to one reported for CoPc grown at RT [21]. The in-plane density of molecules in R33.69 structure is larger (in-plane molecule separation is by ~4%) than one in the 5x5 structure. Interestingly we have found that, the selective nucleation and growth of R33.69 and 5x5 structures are precisely tunable solely by maintaining a substrate temperature without choosing alternate metal center and substrate, for coverages below 1ML. At higher temperatures, if deposition of ZnPc molecules exceeds 1ML, the single crystalline 5x5 phase transforms irreversibly into the R33.69 one, which can have domain sizes of few tens to several hundred μm. Full elucidation of the underlying kinetic factors in tuning of structural phases (conformations) found in this material system requires further detailed study, but our findings provide a new insight in understanding of nucleation and growth of anisotropic organic molecules, and can easily be extended on other similar phthalocyanine-metal systems.

Acknowledgements

We would like to thank Ping Liu and Gary Nintzel for technical support. This research used resources of the Center for Functional Nanomaterials and National Synchrotron Light Source, which are the U.S. DOE Office of Science User Facilities, at Brookhaven National Laboratory under Contract No. DE-SC0012704.

References

[1] J. Michael Gottfried, "Surface chemistry of porphyrins and phthalocyanines", Surface Science Reports **70**, 259 (2015).

[2] R. A. Wassel and C. B. Gorman, Angew. Chem. Int. Ed. **43**, 5120 (2004).

[3] F. I. Bohrer, C. N. Colesniuc, J. Park, M. E. Ruidiaz, I. K. Schuller, A. C. Kummel, and W. C. Trogler, J. Am. Chem. Soc. **131**, 478 (2009).

[4] M. García-Iglesias, J. –J. Cid, J. –H. Yum, A. Forneli, P. Vázquez, M. K. Nazeeruddin, E. Palomares, M. Grätzel, and T. Torres, Energy Environ. Sci. **4**, 189 (2011).

[5] D. Dini and M. Hanack, in: K. M. Kadish, R. Guilard, K. M. Smith (Eds.), The Porphyrin Handbook Vol. **17**, Amsterdam, 1-36 (2003).

[6] O. L. Kaliya, E. A. Lukyanets, and G. N. Vorozhtsov, J. Porphyrins Phthalocyanines **3**, 592 (1999).

[7] W. Li , A. Yu , D. C. Higgins , B. G. Llanos, and Z. Chen, J. Am. Chem. Soc. **132**, 17056 (2010).

[8] A. Loas, R. Gerdes, Y. Zhang, and S. M. Gorun, Dalton Trans. **40**, 5162 (2011).

[9] T. A. Temofonte and K. F. Schoch, J. Appl. Phys. **65**, 1350 (1989).

[10] W. Gopel, Synthetic Metals **41**, 1087 (1991).

[11] M. Bouvet, Anal. Bioanal. Chem. **384**, 366 (2006).

[12] J. Zhou and Q. Sun, J. Am. Chem. Soc. **133**, 15113 (2001).

[13] A. B. Sorokin, Chem. Rev., **113**, 8152 (2013).

[14] N. B. McKeown, Phthalocyanine Materials; Cambridge University Press (1998).

[15] A. Wilson and R. A. Collins, Sensors and Actuators **12**, 389 (1987).

[16] S. Heutz, S. M. Bayliss, R. L. Middleton, G. Rumbles, and T. S. Jones, J. Phys. Chem. **B104**, 7124 (2000).

[17] A. Al-Mahboob, J. T. Sadowski, T. Nishihara, Y. Fujikawa, Q. K. Xue, K. Nakajima and T. Sakurai, Surf. Sci. **601**, 1311 (2007).

[18] A. Al-Mahboob, J. T. Sadowski, Y. Fujikawa, K. Nakajima and T. Sakurai, Phys. Rev. **B77**, 035426 (2008).

[19] J. T. Sadowski, G. Sazaki, S. Nishikata, A. Al. Mahboob, Y. Fujikawa, K. Nakajima, R. M. Tromp and T. Sakurai, Phys. Rev. Lett. **98**, 046104 (2007).

[20] A. Al-Mahboob, Y. Fujikawa, T. Sakurai and J. T. Sadowski, Adv. Func. Mater. **23**, 2653 (2013).

[21] E. Salomon, P. Amsalem, N. Marom, M. Vondracek, L. Kronik, N. Koch and T. Angot, Phys. Rev. **B87**, 075407 (2013).

[22] W. Dou, Y. Tang, C. S. Lee, S. N. Bao, and S. T. Lee, J. Chem. Phys. **133**, 144704 (2010).

[23] B. Stadtmüller, I. Kröger, F. Reinert and C. Kumpf, Phys. Rev. **B 83**, 085416 (2011).

[24] E. Bauer, Rep. Prog. Phys. **57**, 895 (1994).

[25] B. Delley, J. Chem. Phys. **92**, 508 (1990).

[26] B. Delley, J. Chem. Phys. **113**, 7756 (2000).

[27] J. P. Perdew, K. Burke, and M. Ernzerhof, Phys. Rev. Lett. **77**, 3865 (1996).

[28] S. Grimme, J. Comput. Chem. **27**, 1787 (2006).

[29] E. R. McNellis, J. Meyer, and K. Reuter, Phys. Rev. **B80**, 205414 (2009).

[30] D. D. Koelling, and B. N. Harmon, J. Phys. C: Solid State Phys. **10**, 3107 (1977).

[31] M. Douglas and N. M. Kroll, Ann. Phys. (San Diego) **82**, 89 (1974).

[32] B. Delley, Int. J. Quant. Chem. **69**, 423 (1998).

[33] I. Kröger, B. Stadtmüller, C. Wagner, C. Weiss, R. Temirov, F. S. Tautz and C. Kumpf, J. Chem. Phys. **135**, 234703 (2011).

[34] A. Al-Mahboob, Y. Fujikawa, J. T. Sadowski, T. Hashizume and T. Sakurai, Phys. Rev. **B82**, 235421 (2010).

[35] A. Mugarza, R. Robles, C. Krull, R. Korytár, N. Lorente, and P. Gambardella, Phys. Rev. **B85**, 155437 (2012).

Figures' Captions

Figure 1. (a) – (c) Time-series LEEM images obtained during growth of ZnPc on Ag(100) at 375K: (a) before nucleation of crystalline islands at nominal coverage of 0.3M, (b) right after nucleation – 0.35ML, and (c) at 0.7 ML nominal coverage; field-of-view 10μm; E = 2.5eV; and (d) - (e) μ-LEED patterns recorded during the growth of ZnPc: (d) before an onset of nucleation of crystalline islands (0.3 ML) at 375K, E = 2eV; (e) from 1ML ZnPc crystalline islands grown at 375K, E = 4eV and (f) from 1ML ZnPc crystalline islands grown at 460K, E =25eV.

Figure 2. μ-LEED patterns obtained from ZnPc crystalline islands grown at various temperatures: (a) double-domain R33.69 phase grown at 375K with orientations of two domains outlaid on the pattern; (b) single-crystalline 5x5 phase grown at 460K, and (c) LEED pattern from a clean Ag(100) surface as a reference – Ag(100) first-order diffraction spots are marked by yellow circles in (b) and (c). Size of selected-area aperture for μ-LEED was 2μm.

Figure 3. Coverages of ZnPc crystalline phases versus nominal deposition, extracted from real-time LEEM observations of ZnPc deposition on Ag(100) at substrate temperatures of 375K and 520K, respectively.

Figure 4. (a) Side and top views of a ZnPc molecule adsorbed on Ag(100) with schematics of adsorption geometry and possible adsorption sites considered in calculations; (b) A diagram of calculated binding energies of ZnPc molecules having different azimuthal orientations and adsorption sites as marked in (a); a hollow site with ±30° rotation of molecular axis in regard to [011] axis of the substrate is a preferred adsorption configuration.

Figure 5. (a) Critical coverage required for a nucleation of crystalline ZnPc islands at given temperature, for both, R33.69 and 5x5 phases; (b) Arrhenius plots of the data with extracted values of effective bonding energies for each phase.

Figure 6. μ-LEED patterns illustrating the phase transition from 5x5 (left) to R33.69 phase (right) at 460K, when the nominal coverage reaches 1ML; weak satellite spots in the right pattern are from Moiré modulation formed by overlapping ZnPc and Ag crystal lattices; electron energies are 25eV and 23eV, respectively.

Fig. 1

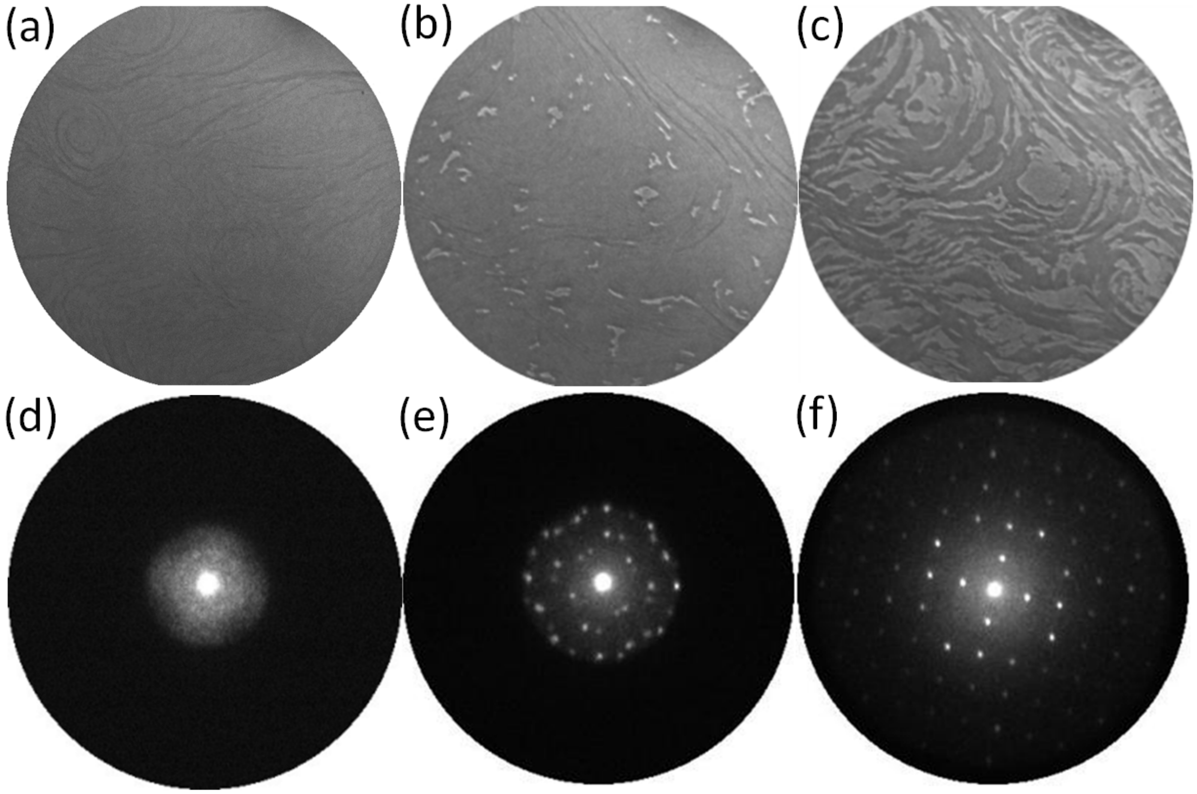

Fig. 2

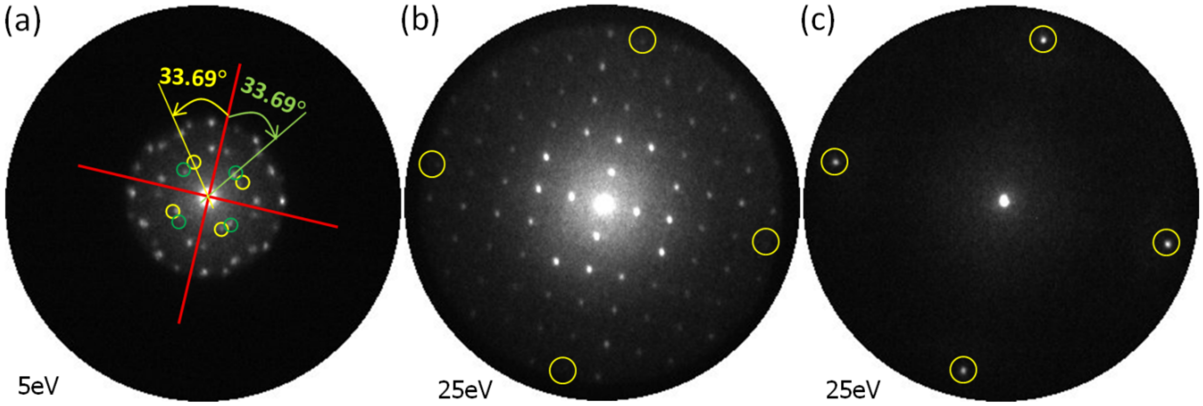

Fig. 3

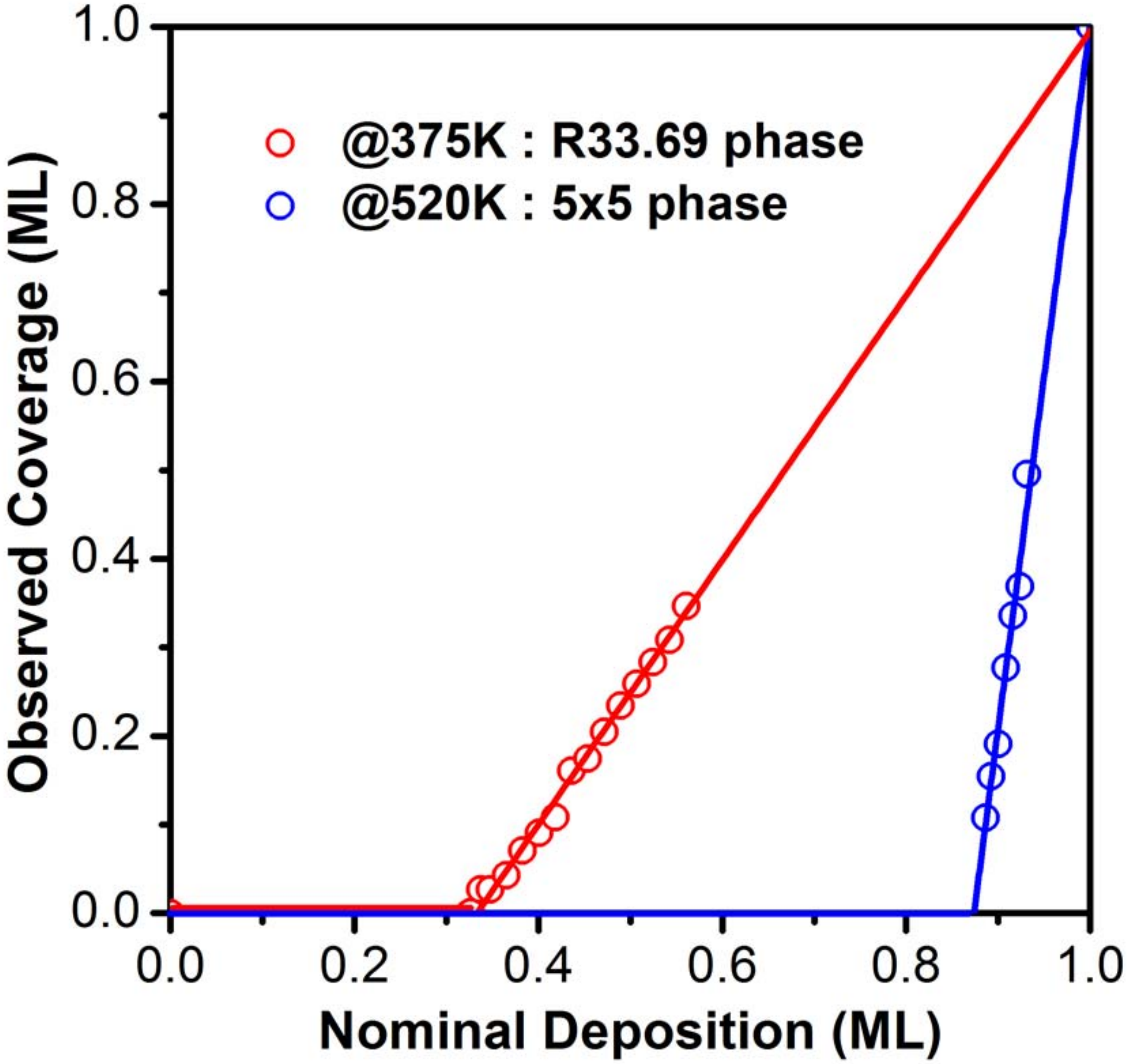
○ @375K : R33.69 phase
○ @520K : 5x5 phase
Observed Coverage (ML)
Nominal Deposition (ML)
0.0
0.2
0.4
0.6
0.8
1.0
0.0
0.2
0.4
0.6
0.8
1.0

Fig. 4

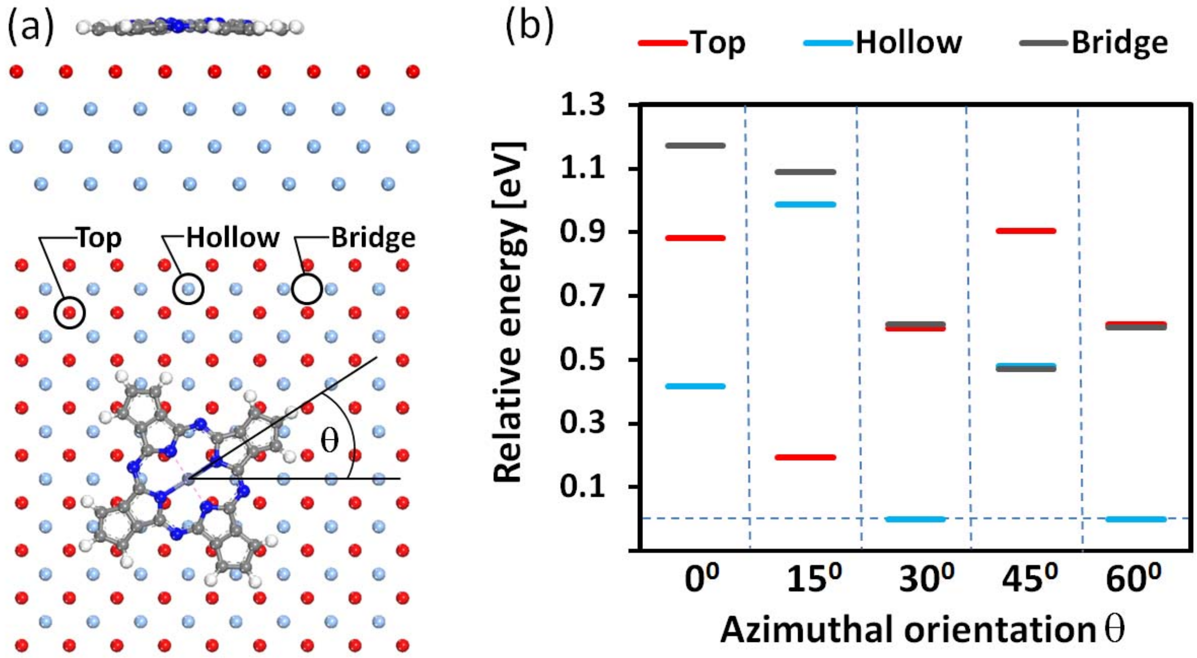
(a)
Top
Hollow
Bridge
θ
(b)
Top
Hollow
Bridge
1.3
1.1
0.9
0.7
0.5
0.3
0.1
Relative energy [eV]
0⁰
15⁰
30⁰
45⁰
60⁰
Azimuthal orientation θ

Fig. 5

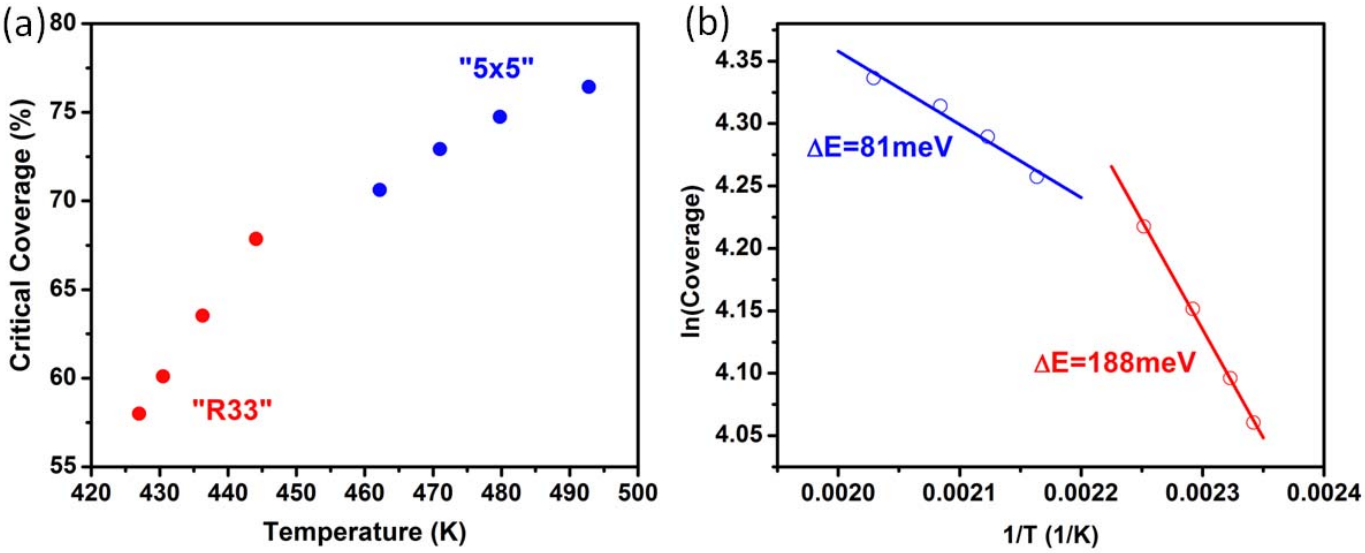
(a)
Critical Coverage (%)
80
75
70
65
60
55
"5x5"
"R33"
420
430
440
450
460
470
480
490
500
Temperature (K)
(b)
ln(Coverage)
4.35
4.30
4.25
4.20
4.15
4.10
4.05
ΔE=81meV
ΔE=188meV
0.0020
0.0021
0.0022
0.0023
0.0024
1/T (1/K)

Fig. 6